Fano resonances GaN-based high contrast grating surface-emitting lasers

Tzeng-Tsong Wu, Shu-Hsien Wu, Tien-Chang Lu, Hao-Chung Kuo and Shing-Chung Wang
Department of Photonics & Institute of Electro-Optical Engineering, National Chiao Tung University,
Hsinchu 30050, Taiwan

ABSTRACT

GaN-based high contrast grating surface-emitting lasers (HCG SELs) with AlN/GaN distributed Bragg reflectors were reported. The device exhibited a low threshold pumping energy density of about 0.56 mJ/cm^2 and the lasing wavelength was at 393.6 nm with a high degree of polarization of 73% at room temperature. The specific lasing mode and polarization characteristics agreed well with the theoretical modeling. The low threshold characteristics of our GaN-based HCG SELs utilized by the Fano resonance can be potential for development of blue surface emitting laser sources

Keywords- GaN, Fano resonance, high contrast grating, surface-emitting laser

1. INTRODUCTION

Sub-wavelength high contrast gratings (HCGs) have been widely investigated in the recent years owing to their advantageous properties. By modification of HCG parameters such as grating height, period and width, high reflectivity reflectors with broad stopband width and specific polarization could be achieved and applied for many applications. [1-5] Owing to the superior properties, the vertical cavity surface-emitting lasers (VCSELs) integrated with the HCGs as the top mirrors which not only serve as high reflectivity reflectors for VCSELs but also provide unique characteristics including polarization selection, wavelength tuning and fast modulation speed. [2, 5]

Being a potential for development of high power surface-emitting lasers (SELs), sub-wavelength HCGs could be employed for high-quality factor (Q) resonators with in-plane oscillation over a large area. [6, 7] In 2008, Zhou *et al*. have demonstrated the GaAs-based membrane HCG high-Q resonators at low temperature, where the GaAs-based membrane HCGs were fabricated by selective etching and e-beam lithography. High Q value of the resonator supported by the Fano resonance [6] was obtained to be 14000 by optical pumping at 4K.

In the development of SELs toward the short wavelength region, GaN-based VCSELs and photonic crystal surface emitting lasers (PCSELs) have received much research attention recently. [8-14] The simple geometry of membrane HCG high-Q resonators can be applied for realizing SELs. However, it is still challenge to fabricate GaN-based membrane HCG structures due to the immature etching process to fabricate realized at room temperature by optical pumping. [15] In this report, we have designed, fabricated and demonstrated the GaN-based HCG SELs with AlN/GaN distributed Bragg reflectors (DBRs). Without using the suspended membrane structure, the AlN/GaN DBRs can play an important role as the low refractive index layer for confining the optical mode in the HCG cavity. Finally, the specific lasing mode was compared to the band diagram and mode pattern calculated by plane wave expansion (PWE) [16] and finite element methods (FEM) [17].

2. SIMULATION

Schematics of GaN-based HCG SELs are shown in Fig. 1(a). We used RCWA to analyze the corresponding asymmetric reflectivity spectra as functions of different duty cycle (the grating width divided by the grating period) and grating height for the TE polarization of the GaN-based HCG. First, the grating period was designed to be 345 nm to bring the Fano resonance approaching to the GaN gain peak. Fig. 1(b) shows the calculated reflectivity spectra mapping as a function of duty cycle. To match the target wavelength of about 400 nm, the duty cycle was set to be around 0.8 to 0.86 for fabrication tolerance. Fig. 1(c) shows the calculated reflectivity spectra mapping versus grating height. The calculated results show the number of reflectivity peaks would increase with increasing the grating height due to the onset of higher

High Contrast Metastructures II, edited by Connie J. Chang-Hasnain, Fumio Koyama, Alan Eli Willner, Weimin Zhou, Proc. of SPIE Vol. 8633, 86330B · © 2013 SPIE
CCC code: 0277-786X/13/$18 · doi: 10.1117/12.2002911

Downloaded From: http://proceedings.spiedigitallibrary.org/ on 04/27/2014 Terms of Use: http://spiedl.org/terms

order Fabry-Perot modes. In order to fit our target wavelength, the grating height was selected to be around 490 to 530 nm which was closed to a 3λ cavity. Fig. 1(d) shows the reflectivity spectrum when the grating period, height and duty cycle were set to be 345 nm, 520 nm (3λ cavity) and 0.82. The reflectivity spectrum shows an asymmetric line shape from 0 to 1 which was referred to the feature of Fano resonance. [5] For GaN-based HCG SELs, the first optical channel is the Bragg scattering induced by HCG in lateral direction, the Bragg scattering would cause the narrow band width spectrum. On the other hand, the second optical channel is the Fabry-Perot scattering induced by index difference in vertical direction, the Fabry-Perot scattering would generate a flat band spectrum. These two different channels would reach the same final state resulting in asymmetric line shape of the spectrum. This phenomenon could confine the optical mode in the structure well and result in a high Q factor which is beneficial for the laser operation. The simulated reflectivity spectrum can be compared to the Fano resonance equation:

$$F(\Omega) = \frac{1}{1+q^2}\frac{(\Omega+q)^2}{\Omega^2+1} \text{ and } \Omega = \frac{2(\omega-\omega_0)}{\gamma}, \quad (1)$$

where ω_0 and γ are the center frequency and the width of the narrowband, q is the Fano asymmetry parameter. The Q factor of the cavity can be calculated by using $Q = \omega_0/\gamma$. The blue curve in Fig. 1(b) representing the fitted Fano resonance curve based on Eq. (1) matches quite well to the simulated reflectivity spectra obtained by RCWA. The extracted Q factor in this case was calculated to be 533.

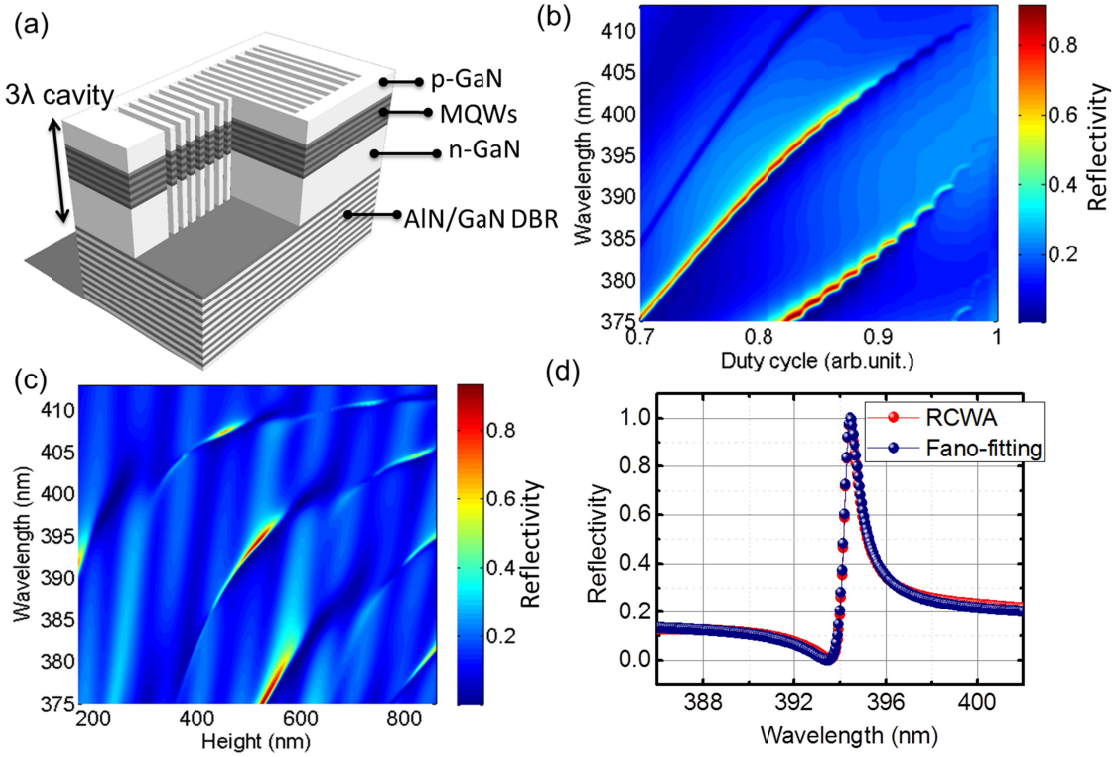

Figure 1 (a) Schematics of GaN-based HCG SELs. (b) Reflectivity spectra mapping as a function of duty cycle (the grating width divided by the grating period). (c) Reflectivity spectra mapping versus grating height. (d) The reflectivity spectra for the grating with period: 345nm, filling factor: 0.82, grating height: 520 nm. The red and navy line show the simulation results by RCWA and fitting results by the Fano resonance equation.

3. EXPERIMENT

In experiment, the GaN-based HCG SELs were grown by a metal-organic chemical vapor deposition (MOCVD) system on a c-plane 2-in sapphire substrate. The epitaxial structure consisted of a 25-pair AlN/GaN DBR, a 320 nm-thick n-GaN layer, 10 pairs of InGaN/GaN multiple quantum wells (MQWs), and a 100 nm-thick p-GaN layer. The typical photoluminescence (PL) spectrum of MQWs had a peak centered at 405 nm with a linewidth of about 25 nm. In the fabrication steps, the as-grown sample was first deposited a 300 nm-thick SiNx layer by plasma-enhanced chemical vapor deposition (PECVD) as the hard mask and spin-coated the poly-methyl methacrylate (PMMA) photoresist. The HCG structure was patterned by electron-beam lithography on the PMMA, and then etched by reactive ion etching (RIE) down

Downloaded From: http://proceedings.spiedigitallibrary.org/ on 04/27/2014 Terms of Use: http://spiedl.org/terms

to SiNx layer. Then, the HCG patterns were etched down to penetrate the MQWs layer of about 490 nm using inductively coupled plasma (ICP) dry etching. The total area of HCG region was about 20 μm^2. Fig. 2 shows the planer and tilted angle scanning electron microscope (SEM) images of the device. It can be seen that the period, duty cycle and height of HCG were estimated to be 345 nm, 0.82 and 490 nm, respectively. The 355 nm pulse Nd:YVO_4 laser with a pulse width of ~0.5 ns at a repetition rate of 1 kHz was used as the optical pumping source in the measurement system. All the experiments were carried out at room temperature. The laser beam pumped obliquely onto the GaN-based HCG SELs devices with a spot size of about 20 μm to cover the HCG pattern. The μ-PL signal was collected by a 15X objective lens normal to the sample surface or by a fiber with a 600 μm core in the normal plane of the sample and fed into a spectrometer with a charge-coupled device(Jobin-Yvon IHR320 Spectrometer). The spectral resolution was about 0.07 nm for spectral output measurement.

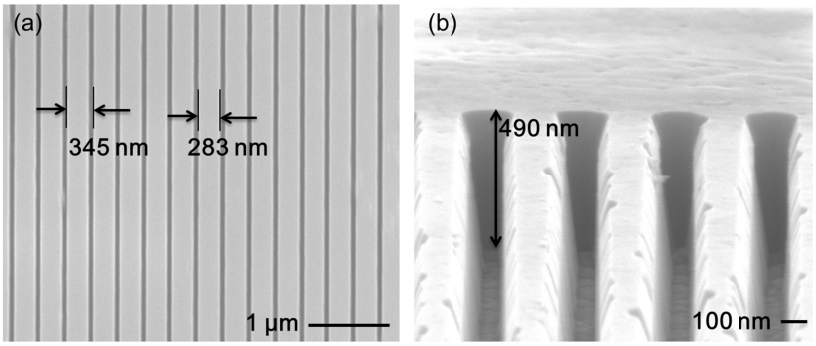

Figure 2 The (a) planer and (b) tilted angle SEM images of GaN-based HCG SELs. The period, duty cycle and height of HCG were estimated to be 345 nm, 0.82 and 490 nm, respectively.

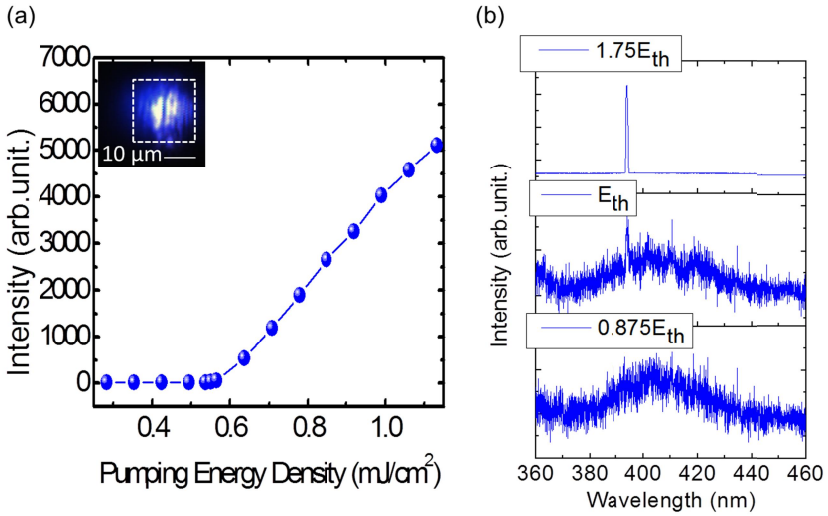

Figure 3 (a) The input-output characteristics of GaN-based HCG SELs. The inset shows the CCD images when the GaN-based HCG SEL was above the threshold condition. (b) The measured spectra with different pumping power of 0.875 E_{th}, E_{th} and 1.75 E_{th}. The full width at half maximum (FWHM) of lasing peak at 1.75 E_{th} is 0.88 nm.

4. RESULTS AND DISCUSSIONS

The pumping energy density versus the output characteristics curve of GaN-based HCG SELs is shown in Fig. 3(a). A clear threshold can be observed when the threshold energy density was about 0.56 mJ/cm^2. Compared to the previous reports, the threshold condition of GaN-based HCG SELs was superior to the GaN-based PCSELs of about 2.7 mJ/cm^2 and GaN-based VCSELs of about 1.15 mJ/cm^2. The ultralow threshold condition can be attributed to the Fano resonance supporting the perfect mode confinement in HCG structures. The right inset of Fig. 3(a) shows the CCD image when the GaN-based HCG SEL was above the threshold condition. The white dash line represents the whole HCG area and it could be discovered that the lasing area covered most of the HCG pattern. Fig. 3(b) shows the lasing spectra with different pumping energy density. When it was above the threshold condition, one dominated lasing peak was observed and located

Downloaded From: http://proceedings.spiedigitallibrary.org/ on 04/27/2014 Terms of Use: http://spiedl.org/terms

at 393.6 nm. The emission spectrum right below the threshold condition of GaN-based HCG SEL is plotted in Fig. 3. The spectrum with black curve exhibits an asymmetric line shape, which is the characteristic of Fano resonance. The Q factor can thus be estimated by fitting the spectrum with the Fano resonance equation described in Eq. (1). The fitted curve is shown in Fig. 3 as the red curve. The extracted Q factor was estimated to be 394, which was closed to the designed value.

In order to further understand the laser characteristics of GaN-based HCG SEL, the degree of polarization (DOP) and divergence angle were measured at the normal direction to the sample surface. Fig. 4(a) shows the measured DOP results. The DOP is defined as $(I_{max}-I_{min})/(I_{max}+I_{min})$ where I_{max} and I_{min} are the maximum and the minimum intensity of the lasing peak. The DOP can be calculated to be 73%. The high DOP of HCG SELs can be attributed to the resonance direction of electrical fields only parallel to the grating bar. Fig. 4(b) describes the angle versus measured output intensity. The output intensity was collected by a fiber with a 600 μm core normal to the sample surface on the rotational stage. The angle resolution of the rotation stage was about 0.5 degree for divergence angle measurement. The divergence angle of GaN-based HCG SEL was measured to be 12°.

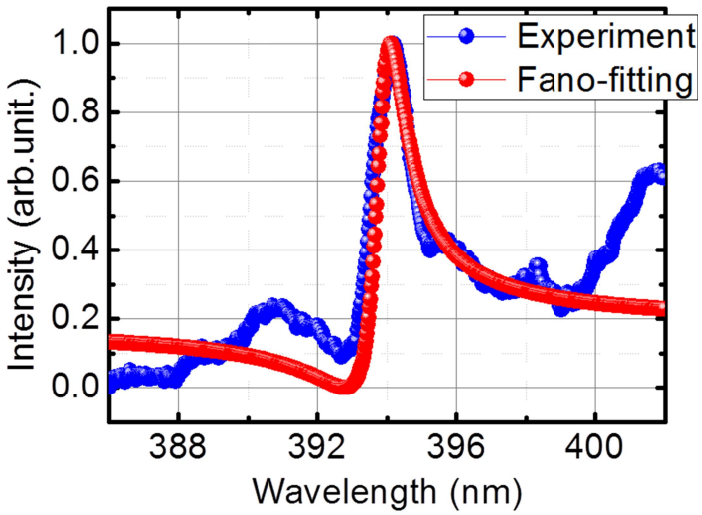

Figure 4 The PL spectra (blue curve) of GaN-based HCG SELs when it was below the threshold condition. The red curve shows the fitting result by Fano-resonance equation. The Q factor was calculated to be 394.

Since the HCG structure can be treated as one dimensional photonic crystal, we can use the PWE method to simulate the photonic band structure of our GaN-based HCG SEL as shown in Fig. 5(a). The normalized frequency of the experimental lasing mode of our GaN-based HCG SEL was located at 0.877, corresponding to the fourth order band in the lower band-edge position in Fig. 5(a). The Bragg scattering of surface emission would occur when the group velocity approached to zero in the fourth order band. The lower band-edge position reveals the resonance mode in the HCG could be identified as the anti-symmetric mode. On the contrary, the symmetric mode would only show the nodes in one grating bar. In addition, the FEM was also used to calculate the mode pattern of GaN-based HCG SEL, as shown in Fig. 5(b). The mode pattern shows several nodes and antinodes which can be referred to the anti-symmetric mode. The simulation also indicates the AlN/GaN DBRs could provide the mode confinement in the HCG cavity. The resonance direction of electric field is parallel to the grating bar which can also confirm the DOP results. Furthermore, the anti-symmetric mode would provide perfectly mode confinement in HCG, resulting in destructive interference in the far-field with little output coupling [7]. The perfect mode confinement supported by Fano resonance could facilitate the high Q factor and the ultralow threshold condition of GaN-based HCG SELs achieved in this experiment.

Downloaded From: http://proceedings.spiedigitallibrary.org/ on 04/27/2014 Terms of Use: http://spiedl.org/terms

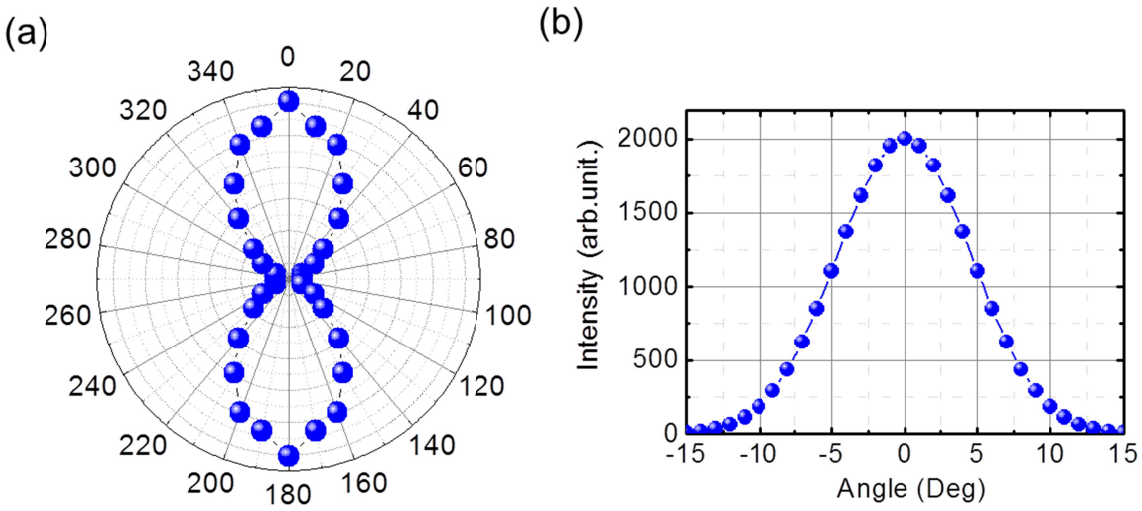

Figure 5 (a) The degree of polarization (DOP) and (b) the divergence angle of the GaN-based HCG SEL when it was above the threshold condition. The detection direction was normal to the surface of the GaN-based HCG SEL. The DOP and divergence angle were measured to be 73% and 12°, respectively.

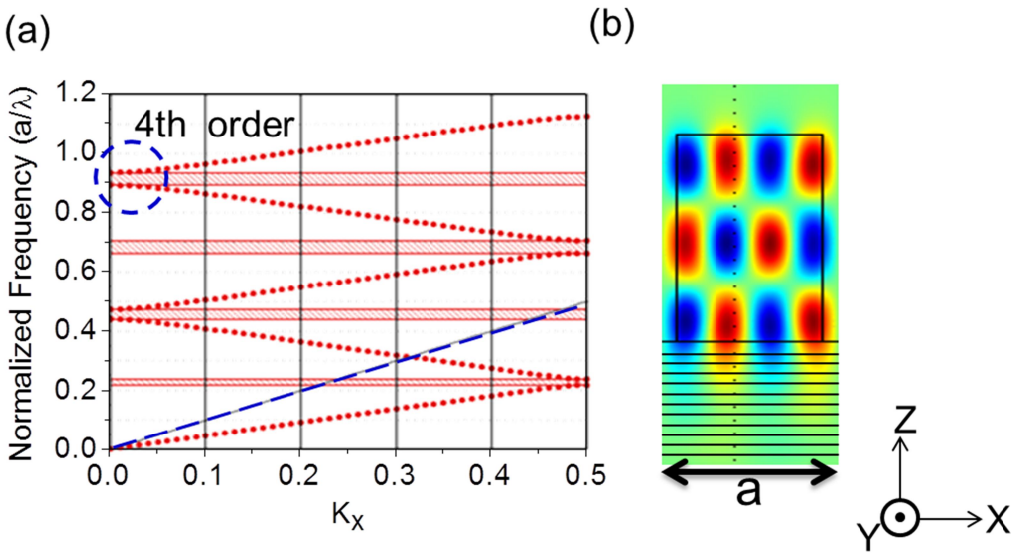

Figure 6 (a) The calculated band structure of GaN-based HCG SEL using the PWE method. The blue dashed line represents the light line. The red dot lines represent the different order bands and the blue circle indicates the forth order band. (b) The calculated mode pattern of GaN-based HCG SEL using the finite element method. The parameter a is the grating period.

5. CONCLUSION

In summary, GaN-based HCG SELs with AlN/GaN DBRs were demonstrated and investigated at room temperature. Supporting by the Fano resonance, the ultralow threshold energy density was measured to be 0.56 mJ/cm^2 and the lasing wavelength was located at 393.6 nm. The asymmetric PL spectrum was observed indicating the Fano resonance phenomenon and the quality factor was extracted to be 394. Furthermore, the lasing characteristics such as the divergence angle and degree of polarization were measured to be 12° and 73%, respectively. Finally, the specific surface emitting lasing mode conformed to the one dimensional photonic band diagram and mode pattern. Since GaN-based SELs have drawn much attention due to many practical applications such as laser display, laser printer, high density optical storage, and the next generation micro/pico-projectors, we believe the GaN-based HCG SELs have the great potential for accomplishment of low threshold, high power short wavelength coherent light sources in the near future.

Downloaded From: http://proceedings.spiedigitallibrary.org/ on 04/27/2014 Terms of Use: http://spiedl.org/terms

ACKNOWLEDGMENT

The authors would like to gratefully acknowledge Prof. Koyama at Tokyo Institute of Technology for his fruitful suggestion. This work was supported in part by the Ministry of Education Aim for the Top University program and by the National Science Council of Taiwan under Contract No. NSC99-2622-E009-009-CC3 and NSC98-2923-E-009-001-MY3.

REFERENCES

[1] C. F. R. Mateus, M. C. Y. Huang, Y. Deng, A. R. Neureuther and C. J. Chang-Hasnain, "Broad-band mirror (1.12-1.62 μm) using a subwavelength grating," IEEE Photon. Technol. Lett 16, 518 (2004).

[2] M. C. Y. Huang, Y. Zhou and C. J. Chang-Hasnain, "A surface-emitting laser incorporating a high-index-contrast subwavelength grating," Nat. Photonics 1, 119 (2007).

[3] M. C. Y. Huang, Y. Zhou and C. J. Chang-Hasnain, "A nanoelectromechanical tunable laser," Nat. Photonics 2, 180 (2008).

[4] V. Karagodsky, B. Pesala, C. Chase, W. Hofmann, F. Koyama and C. J. Chang-Hasnain, "Monolithically integrated multi-wavelength VCSEL arrays using high-contrast gratings," Opt. Express 18, 694 (2010).

[5] C. Chase, Y. Rao, W. Hofmann and C. J. Chang-Hasnain, "1550 nm high contrast grating VCSEL," Opt. Express 18, 15461 (2010).

[6] Y. Zhou, M. C. Y. Huang, C. Chase, V. Karagodsky, M. Moewe, B. Pesala, F. G. Sedgwick and C. J. Chang-Hasnain, "High-index-contrast grating (HCG) and its applications in optoelectronic devices," IEEE J. Sel. Top. Quantum Electron. 15, 1485 (2009).

[7] Y. Zhou, M. Moewe, J. Kern, M. C. Y. Huang and C. J. Chang-Hasnain, "1550 nm high contrast grating VCSEL," Opt. Express 16, 17282 (2008).

[8] T. C. Lu, S. W. Chen, T. T. Wu, P. M. Tu, C. K. Chen, C. H. Chen, Z. Y. Li, H. C. Kuo and S. C. Wang, "Continuous wave operation of current injected GaN vertical cavity surface emitting lasers at room temperature," Appl. Phys. Lett. 97, 071114 (2010).

[9] T. C. Lu, T. T. Wu, S. W. Chen, P. M. Tu, Z. Y. Li, C. K. Chen, C. H. Chen, H. C. Kuo, S. C. Wang, H. W. Zan and C. Y. Chang, "Characteristics of Current Injected GaN-Based Vertical-Cavity Surface-Emitting Lasers," IEEE J. Sel. Top. Quantum Electron. 17, 1594 (2011).

[10] D. Kasahara, D. Morita, T. Kosugi, K. Nakagawa, J. Kawamata, Y. Higuchi, H. Matsumura and T. Mukai, "Demonstration of Blue and Green GaN-Based Vertical-Cavity Surface-Emitting Lasers by Current Injection at Room Temperature," Appl. Phys. Express 4, 072103 (2011).

[11] H. Matsubara, S. Yoshimoto, H. Saito, Y. Jianglin, Y. Tanaka and S. Noda, "GaN photonic-crystal surface-emitting laser at blue-violet wavelengths, " Science 319, 445 (2008).

[12] T. C. Lu, S. W. Chen, L. F. Lin, T. T. Kao, C. C. Kao, P. Yu, H. C. Kuo, S. C. Wang and S. H. Fan, "GaN-based two-dimensional surface-emitting photonic crystal lasers with AlN/GaN distributed Bragg reflector," Appl. Phys. Lett. 92, 011129 (2008).

[13] T. T. Wu, P. S. Weng, Y. J. Hou and T. C. Lu, "GaN-based photonic crystal surface emitting lasers with central defects," Appl. Phys Lett. 99, 221105 (2011).

[14] S. Kawashima, T. Kawashima, Y. Nagatomo, Y. Hori, H. Iwase, T. Uchida, K. Hoshino, A. Numata and M. Uchida, "GaN-based surface-emitting laser with two-dimensional photonic crystal acting as distributed-feedback grating and optical cladding," Appl. Phys. Lett. 97, 251112 (2010).

[15] J. Kim, D. U. Kim, J. H. Lee, H. S. Jeon, Y. S. Park and Y. S. Choi, "AlGaN membrane grating reflector," Appl. Phys. Lett. 95, 021102 (2009).

[16] S. H. Kwon, H. Y. Ryu, G.-H. Kim, Y. H. Lee and S. B. Kim, "Photonic bandedge lasers in two-dimensional square-lattice photonic crystal slabs," Appl. Phys. Lett. 83, 3870 (2003).

[17] J. Jin, The Finite Element Method in Electromagnetics, (Wiley, New York, 2002).

[18] M. G. Moharam and T. K. Gaylord, "Rigorous coupled-wave analysis of planar-grating diffraction," J. Opt. Soc. Am. 71, 811 (1981)

[19] U. Fano, "Effects of Configuration Interaction on Intensities and Phase Shifts, " Phys. Rev. 124, 1866 (1961).

[20] M. V. Rybin, M. V. Rybin, A. B. Khanikaev, M. Inoue, A. K. Samusev, M. J. Steel, G. Yushin and M. F. Limonov, "Bragg scattering induces Fano resonance in photonic crystals," Photonics and Nanostructures–Fundamentals and Applications 8, 86 (2010).

[21] S. L. Chua, Y. D. Chong, A. Douglas Stone, M. Soljačić and J. Bravo-Abad, "Low-threshold lasing action in photonic crystal slabs enabled by Fano resonances," Opt. Express 19, 1539 (2011).

Downloaded From: http://proceedings.spiedigitallibrary.org/ on 04/27/2014 Terms of Use: http://spiedl.org/terms